



Published in final edited form as:

J Biomed Mater Res A. 2015 February ; 103(2): 646–657. doi:10.1002/jbm.a.35204.

Viscoelastic Properties of Collagen-Adhesive Composites under Water Saturated and Dry Conditions

Viraj Singh^{1,3}, Anil Misra^{2,3}, Ranganathan Parthasarathy^{3,4}, Qiang Ye³, and Paulette Spencer^{1,3}

¹Mechanical Engineering Department, University of Kansas, Lawrence

²Civil, Environmental and Architectural Engineering Department, University of Kansas, Lawrence

³Bioengineering Research Center, University of Kansas, Lawrence

⁴Bioengineering Graduate Program, University of Kansas, Lawrence

Abstract

To investigate the time and rate dependent mechanical properties of collagen-adhesive composites, creep and monotonic experiments are performed under dry and wet conditions. The composites are prepared by infiltration of dentin adhesive into a demineralized bovine dentin. Experimental results show that for small stress level under dry conditions, both the composite and neat adhesive have similar behavior. On the other hand, in wet conditions, the composites are significantly soft and weak compared to the neat adhesives. The behavior in the wet condition is found to be affected by the hydrophilicity of both the adhesive and collagen. Since the adhesive-collagen composites are a part of the complex construct that forms the adhesive-dentin interface, their presence will affect the overall performance of the restoration. We find that Kelvin-Voigt model with at least 4-elements is required to fit the creep compliance data, indicating that the adhesive-collagen composites are complex polymers with several characteristic time-scales whose mechanical behavior will be significantly affected by loading rates and frequencies. Such mechanical properties have not been investigated widely for these types of materials. The derived model provides an additional advantage that it can be exploited to extract other viscoelastic properties which are, generally, time consuming to obtain experimentally. The calibrated model is utilized to obtain stress relaxation function, frequency-dependent storage and loss modulus, and rate dependent elastic modulus.

Keywords

collagen-adhesive composite; dentin adhesive; demineralized dentin; creep; viscoelastic; dry and wet; generalized Kelvin-Voigt model

1. Introduction

The composites formed by infiltration of synthetic polymer resins into collagen matrices are common to many biomechanical applications, such as tissue adhesives^{1,2}, collagen based scaffold materials³⁻⁵ and restorative dentistry⁶. Particularly, in restorative dentistry, the dentin adhesive is expected to infiltrate the collagen matrix obtained by demineralizing dentin substrate using acid-etching and undergo in situ polymerization to form a solid collagen-adhesive composite. The composition of the bonding substrate following acid-etching is 30% collagen and 70% water⁷. This collagen-adhesive composite in restorative dentistry is characteristically identified as the hybrid layer and is a major component of adhesive-dentin (a-d) interface. Ideally, the hybrid layer serves as a durable connection between the bulk adhesive and subjacent mineralized dentin. In the mouth, the hybrid layer formed at the a-d interface is subjected to a combination of caustic environment and mechanical loading.

The a-d interface is arguably, the weakest link in composite tooth restorations^{6,8-10}. The loss of integrity of this interface, even in cases in which the restoration remains normally in-place, is clinically relevant because the micro-scale gaps will be infiltrated by enzymes, bacteria and oral fluids. The penetration of these agents into the spaces between the dentin and the composite will lead to recurrent caries, hypersensitivity, pulpal inflammation, and will eventually undermine the restoration. Irrespective of the mechanism by which the restoration fails, the collagen-adhesive composite plays a vital role in load transfer and maintenance of the mechanical integrity of the a-d interface¹¹⁻¹³.

Traditionally, the mechanical behavior of the a-d interface has been investigated using bond strength tests. The bond strength tests treat the dentin-adhesive bond as an integrated entity. The bond strength investigations by nature incorporate the characteristics of dentin, the exposed demineralized dentin collagen, the collagen-adhesive composite, the adhesive in the form of tags or as an intermediate layer, the adhesive-dental composite interface and the dental composite¹⁴⁻¹⁷. However, the construct formed by these various components is quite complex especially, in the proximity of the a-d interface. Therefore, the bond strength tests seldom provide insight into the role played by each of the components that make up this important interface. Bond strength tests also ignore the rate and time dependent behavior of the dentin adhesive and the hybrid layer. Clearly, there are intrinsic merits to understanding how these components perform individually as these insights can be used to better engineer the a-d interface. In our previous work, we reported on the mechanical behavior of the dentin adhesive and the various phases it forms when polymerized in the presence of water under different loading conditions and moisture exposure¹⁸⁻²¹. In this paper, we focus upon the viscoelastic behavior of the collagen-adhesive composites, under conditions that simulate the wet functional environment found in the oral cavity. These collagen-adhesive composites form a major component of the a-d interface and are critical for its long term durability. Currently, limited contradictory experimental results of a subset of mechanical properties have been presented for dentin adhesive infiltrated demineralized dentin²²⁻²⁶. In particular creep and rate-dependent behavior have been rarely examined.

In this work, ideal collagen-adhesive composite are prepared under *in vitro* conditions by the infiltration of dentin adhesive into a collagen matrix obtained by the complete demineralization of bovine dentin. Two types of dentin adhesives with different hydrophilicity are used for the infiltration of demineralized bovine dentin. Further to obtain the time and rate dependent properties of these ideal collagen-adhesive composites creep and monotonic tests are performed in dry and wet conditions. The obtained time and rate dependent properties are compared with those of the neat dentin adhesives. Test results shows that the behavior of collagen-adhesive composite is much more significantly affected by water than the neat adhesive. A linear viscoelastic model for collagen-adhesive composite and dentin adhesives is developed. The applicability and significance of the linear viscoelastic model is demonstrated by predicting stress relaxation behavior, frequency dependent storage and loss moduli and rate dependent elastic modulus.

2. Materials and Methods

2.1. Preparation of Adhesive-Infiltrated Demineralized Bovine Dentin (AIDBD) or Ideal Collagen-Adhesive Composite

2.1.1 Demineralized Bovine Dentin (DBD)—Bovine teeth were sectioned along buccal lingual plane into 15mm long, 1mm thick and 2mm wide slabs using low-speed water-cooled diamond saw (Buehler Ltd, Lake Bluff, IL, USA). Prior to demineralization, the dentin slabs were stored in PBS with sodium azide to prevent any bacterial contamination or growth. The dentin slabs were demineralized in 0.5M EDTA (pH 7.3) at 25° C for 10 days. The solution was changed and samples were washed with distilled water every 24 hours to remove the dissolved mineral. Raman spectra were acquired before the start of the demineralization process. Schematic of various steps involved in obtaining and testing of AIDBD samples is shown in Figure 1. To determine if the demineralization was complete, Raman spectra were collected from the specimens after the 10 days of exposure to EDTA. These spectra were collected from various depths along an exposed section cut from a randomly selected sacrificial sample as shown in inset of Figure 4. The spectra collected prior to and following EDTA storage were compared. The absence of the mineral peak (P-O band at 960cm^{-1}) indicated complete demineralization. It was determined that after 10 days the mineral peak had completely disappeared which agrees with our previous demineralization experience²⁷. Demineralized bovine dentin (DBD) slabs were kept in 70, 95 and 100% ethanol each for 12 hours to gradually replace the water with ethanol.

2.1.2 Adhesive Infiltration—For the adhesive infiltration, we used two adhesive formulations, (a) formulation-1:consisting of 2-Hydroxyethylmethacrylate (HEMA, Acros Organics, NJ) and 2,2-bis[4- (2-hydroxy-3-methacryloxypropoxy) phenyl]-propane (BisGMA, Polysciences, Warrington, PA) with a mass ratio of 45/55 (HEMA/BisGMA) and (b) formulation-2: consisting of HEMA, BisGMA and 2-((1,3-bis(methacryloyloxy)propan-2-yloxy)carbonyl)benzoic acid (BMPB, synthesized by our group)²⁸ with a mass ratio of 45/30/25. The following photoinitiators (all from Aldrich, Milwaukee, WI) were added to both of the adhesives: camphorquinone (CQ), ethyl-4-(dimethylamino) benzoate (EDMAB) and diphenyliodonium hexafluorophosphate (DPIHP). The amounts of photosensitizer, co-initiator amine and iodonium salt were fixed at 0.5 mass

% with respect to the total amount of monomer. All the materials in this study were used as received.

The adhesive formulations were diluted with ethanol in 60/40 weight ratio. The DBD samples were then immersed in the adhesive ethanol mixtures, and stored for 72 hours in a dark room. After 72 hours in the dark, the samples were desiccated in a vacuum oven for 24 hours to remove the solvent. After complete infiltration, adhesive-infiltrated demineralized bovine dentin (AIDBD) samples were polymerized using LED light curing unit of irradiance $250\text{mW}/\text{cm}^2$ and area 6.25mm^2 for 40 seconds (LED Curebox, Proto-tech, and Portland, OR, USA). The polymerized samples were stored in the dark at room temperature for 48 hours to provide adequate time for post-cure polymerization. The AIDBD samples were stored for 72 hours in a vacuum oven in the presence of a drying agent at 37°C to remove water that may have been absorbed during sample preparation.

2.2 Neat Resin (NR) Samples

Rectangular beam samples of cross sections $1\text{mm} \times 1\text{mm}$ and length 15mm of neat adhesive for both the control and experimental formulations were made by curing the adhesive in a glass-tubing mold (Fiber Optic Center Inc, #CV1012, Vitrocom Rectangular Capillary Tubing of Borosilicate Glass)²⁸.

2.3 Degree of Conversion

The degree of conversion (DC) of the AIDBD (collagen-adhesive composite) and neat resin samples was determined using Raman spectroscopy. Spectra were collected using a LabRAM ARAMIS Raman spectrometer (LabRAM HORIBA Jobin Yvon, Edison, New Jersey) with a HeNe laser ($\lambda=633\text{ nm}$, a laser power of 17 mW) as an excitation source. To determine the DC, spectra of the uncured resins and polymerized samples were acquired over a spectral range of $700 - 1800\text{ cm}^{-1}$. The change of the band height ratios of the aliphatic carbon-carbon double bond (C=C) peak at 1640 cm^{-1} and the aromatic C=C at 1610 cm^{-1} (phenyl) in both the cured and uncured states was monitored²⁹. DC was calculated using the following formula based on the decrease in the intensity band ratios before and after light curing:

$$DC (\%) = 100[1 - (R_{\text{cured}}/R_{\text{uncured}})], R = (\text{band height at } 1640\text{ cm}^{-1}/\text{band height at } 1610\text{ cm}^{-1})$$

2.4 Volumetric Composition

Two randomly selected DBD samples were measured for their wet weight M_{wet} . The samples were then dehydrated in vacuum chamber to remove the free water and their dry weight determined as M_{dry} . The water mass fraction of DBD was calculated as $\gamma_w = (M_{\text{wet}} - M_{\text{dry}})/M_{\text{wet}}$.

The collagen and dentin adhesive mass and volume fractions in AIDBD were obtained as follows:

1. The DBD sample used for dentin adhesive infiltration was first weighed in its wet state to find the wet weight, S_{wet} . Thus the dry weight of DBD was then determined as, $S_{dry} = (1 - \gamma_w)S_{wet}$, where w is the water mass fraction.
2. Subsequently, the DBD sample was infiltrated with dentin adhesive and polymerized to form the AIDBD sample, which was used to obtain the dry weight P_{dry} . The AIDBD sample was saturated with water to obtain wet weight P_{wet} . The mass fractions γ_a and γ_c of adhesive and collagen, respectively, in wet AIDBD

$$\text{were obtained as follows, } \gamma_a = \frac{P_{dry} - S_{dry}}{P_{wet}}, \gamma_c = \frac{S_{dry}}{P_{wet}}$$

3. The volume fraction of collagen in wet AIDBD is then calculated using the following relation: $\phi_c = 1 - \phi_w - \phi_a$, where, ϕ_a and ϕ_w are the volume fractions of adhesive and water, respectively, in wet AIDBD. The volume fraction of adhesive and water are estimated using the following relations:

$$\phi_a = \frac{P_{dry} - S_{dry}/\rho_{dry}^a}{P_{wet}/\rho_{wet}^{AIDBD}}, \phi_{water} = \frac{P_{wet} - P_{dry}}{P_{wet}/\rho_{wet}^{AIDBD}}, \text{ where } \rho_{dry}^a \text{ and } \rho_{wet}^{AIDBD} \text{ are the density of dry adhesive and wet AIDBD samples, respectively.}$$

2.5 Mechanical Tests

2.5.1 Mechanical Instrument and Data Interpretation—To obtain the mechanical properties of AIDBD and NR in dry and water-submerged conditions, creep and monotonic tests were performed using universal testing machine (Bose Electroforce 3200, Bose Corporation, Electroforce System Group, Eden Prairie, Minnesota, USA) in a 3-point bending configuration with 10 mm span. Monotonic tests were carried out at the displacement rate of 60 $\mu\text{m}/\text{min}$ ¹⁹. The creep tests were performed on AIDBD and NR samples under the small stress amplitude of 4.5MPa in dry and wet conditions^{18,19}. During creep experiments, the loading is applied as a ramp with a rate of 9 N/min, such that the stress amplitude of 4.5MPa is achieved in ~2 seconds beyond which the stress is held constant. This loading rate is approximately 100 times faster than the monotonic tests. Monotonic tests were also performed on the demineralized bovine dentin (DBD) sample using a tensile clamp but only in the wet environment. Before conducting mechanical tests under wet conditions both the AIDBD and NR samples were stored in water for at least 5 days for complete saturation. Further, to compute the stress and strain from the flexural load-displacement data elastic beam theory was used. The sample size for each test in this study was fixed at $n=3$ and all the tests were performed at room temperature.

2.5.2. Linear Viscoelastic Model—The linear viscoelastic response of AIDBD and NR was modeled using a generalized Kelvin-Voigt representation with 4 elements^{30,31} as shown in Figure 2. The governing equation for the model is given as follows:

$$\varepsilon(t) = \left(\frac{1}{E_0} + \frac{1}{E_1 + \mu_1 \frac{\partial}{\partial t}} + \frac{1}{E_2 + \mu_2 \frac{\partial}{\partial t}} + \frac{1}{E_3 + \mu_3 \frac{\partial}{\partial t}} + \frac{1}{E_4 + \mu_4 \frac{\partial}{\partial t}} \right) \sigma(t) \quad (1)$$

Here, E_0, E_1, E_2, E_3, E_4 , are the spring constants and μ_1, μ_2, μ_3 and μ_4 are the viscosities associated with each element of the model in Figure 2. To obtain the solution of the above differential equation either stress history or strain history is specified. For a constant stress history i.e. $\sigma = \sigma_0$, the following solution to Eq(1) is obtained using Laplace transformation

$$\varepsilon(t) = J(t)\sigma_0 \quad (2)$$

In Eq(2), $J(t)$ is the creep compliance function which takes the following form:

$J(t) = J_0 + J_1(1 - e^{-\frac{t}{\tau_1}}) + J_2(1 - e^{-\frac{t}{\tau_2}}) + J_3(1 - e^{-\frac{t}{\tau_3}}) + J_4(1 - e^{-\frac{t}{\tau_4}})$ where compliance coefficients, $J_0 = \frac{1}{E_0}$; $J_i = \frac{1}{E_i}$ and $\tau_i = \frac{\mu_i}{E_i}$ and $i = 1 \dots 4$. For the numerical calculations, the retardation times $\tau_1, \tau_2, \tau_3, \tau_4$ were taken to be *1min, 10min, 100min* and *1000min* respectively. Equation 2 is often termed as Prony series. Similar to a constant stress history, for a constant strain loading i.e. $\varepsilon = \varepsilon_0$, the stress σ is related to strain ε through a relaxation function $G(t)$ as:

$$\sigma(t) = G(t)\varepsilon \quad (3)$$

here, $G(t) = G_0 + G_1(1 - e^{-\frac{t}{\tau_1}}) + G_2(1 - e^{-\frac{t}{\tau_2}}) + G_3(1 - e^{-\frac{t}{\tau_3}}) + G_4(1 - e^{-\frac{t}{\tau_4}})$ and relaxation constants G_0, G_1, G_2, G_3, G_4 and relaxation times $\tau_1, \tau_2, \tau_3, \tau_4$ are complex function of spring stiffness and damper viscosities. Therefore G_0, G_1, G_2, G_3, G_4 and $\tau_1, \tau_2, \tau_3, \tau_4$ are computed numerically in the current work.

Also the constitutive equation given in differential form in Eq(1) can be written in integral form using either creep compliance or stress relaxation function. If compliance function $J(t)$ is known constitutive equation is represented as follows

$$\varepsilon(t) = J(t)\sigma(0) + \int_0^t J(t-s) \frac{d\sigma(s)}{ds} ds \quad (4)$$

On the other hand, if relaxation function $G(t)$ is known constitutive equation takes the following form:

$$\sigma(t) = G(t)\varepsilon(0) + \int_0^t G(t-s) \frac{d\varepsilon(s)}{ds} ds \quad (5)$$

During the creep test, constant stress is applied, therefore, $\frac{d\sigma(t)}{dt} = 0$ in Eq(4) whereas, in a strain controlled monotonic test, strain is applied at a constant rate, that is $\frac{d\varepsilon(t)}{dt} = k$ in Eq(5), where k is the rate of loading. In addition, the creep compliance function $J(t)$, can be used to compute the dynamic properties if sinusoidal stress history is applied such that

$$\sigma(t) = \sigma_0 \sin \omega s \quad (6)$$

Here, σ_0 is the stress amplitude and $\omega=2f\pi$, where f is the loading frequency. Substituting the dynamic stress given in Eq (6) into Eq(4) and simplifying, the real and imaginary part of creep compliance, J' and J'' , are obtained as follows

$$J' = J_\infty - \frac{J_1(\omega\tau_1)^2}{1+(\omega\tau_1)^2} - \frac{J_2(\omega\tau_2)^2}{1+(\omega\tau_2)^2} - \frac{J_3(\omega\tau_3)^2}{1+(\omega\tau_3)^2} - \frac{J_4(\omega\tau_4)^2}{1+(\omega\tau_4)^2} \quad (7)$$

where $J_\infty = J_0 + J_1 + J_2 + J_3 + J_4$

$$J'' = -\frac{J_1(\omega\tau_1)}{1+(\omega\tau_1)^2} - \frac{J_2(\omega\tau_2)}{1+(\omega\tau_2)^2} - \frac{J_3(\omega\tau_3)}{1+(\omega\tau_3)^2} - \frac{J_4(\omega\tau_4)}{1+(\omega\tau_4)^2} \quad (8)$$

Now, the loss moduli G' and G'' can be obtained as follows

$$G' = \frac{J'}{(J')^2 + (J'')^2} \quad (9)$$

$$G'' = \frac{J''}{(J')^2 + (J'')^2} \quad (10)$$

Finally, $\tan(\delta)$ can be obtained from loss and storage modulus as $\tan\delta = \frac{G''}{G'}$

3. Results

3.1 Raman Spectroscopy and Degree of Conversion

Raman spectra were acquired on the randomly collected bovine dentin slabs before the start of demineralization process to identify the spectral features associated with mineral (P-O band at 960cm^{-1}) and collagen (amide I C=O 1653cm^{-1}). Figure 3 shows the Raman spectra with the normalized intensity acquired at different locations on the bovine dentin samples. Because of the concentration of mineral, the mineral peak dominates the amide I peak. After demineralization, the Raman spectra, given in Figure 4, show an absence of the P-O peak at 960cm^{-1} and strong presence of amide I peak at 1653cm^{-1} . This indicates complete demineralization of the bovine dentin slabs.

The adhesive infiltration in the AIDBD samples was determined by acquiring Raman spectra across the cross-section of randomly selected samples. Raman spectra for both the control and the experimental formulations are shown in Figure 5. The presence of spectral feature associated with the dentin adhesive (aliphatic C=C, peak at 1640cm^{-1} and the aromatic C=C at 1610cm^{-1}) across the cross-section indicated complete infiltration. The interference of amide I peak at 1653cm^{-1} was removed while calculating the degree of conversion. The measured degree of conversion was found to be $87.0\%(\pm 0.5)\%$ and $84.4\%(\pm 2.1)\%$ for the AIDBD samples of control and experimental formulations, respectively. We note that the degree of conversion for the control and experimental neat resin samples was $90.0\%(\pm 1.5)\%$ and $88.0\%(\pm 1.25)\%$, respectively.

3.2 Volumetric and Mass Composition

Calculated weight and volume fractions of DBD and dentin adhesive present in wet AIDBD are given in Table 1. Based upon the mass change study, the amount of water present in DBD samples was 50% ($\pm 0.3\%$). Further for the calculation of volume fractions, densities of dry adhesive and wet AIDBD are taken to be 1.2g/cm^3 and 1.1g/cm^3 respectively. The volume fraction for adhesive and collagen in wet state was found to be 42.12% ($\pm 1.10\%$) and 43.33% ($\pm 1.14\%$) respectively.

3.3 Mechanical Tests

The results of the creep tests on AIDBD and NR samples in dry and wet condition are shown in Figure 6 a-d. From Figure 6a we observe that in the dry condition, the creep curves for both NR formulations were identical. The strain at the end-of-loading, considered at time $t=0$, was 0.2%, and the creep strain reached an asymptote of 0.35% in 1440 minutes (24hrs). The creep behavior of AIDBD in dry condition was similar to that of NR, strain at the end-of-loading was $\sim 0.25\%$ and the creep strain reached an asymptote of $\sim 0.40\%$ in 24 hours for both AIDBD samples. On the other hand, in the wet condition the NR samples have end-of-loading strain of 0.32% and 0.35%, and asymptotic creep strain of 0.67% and 0.88%, for formulations 1 and 2 respectively. Whereas, the AIDBD-1 and AIDBD-2 have end-of-loading strain of 0.60% and 0.81%, and asymptotic creep strain of 1.18% and 1.66%, respectively. Creep data is also plotted on a log-log plot in Figures 6c and 6d. The presence of inflection points in the log-log plot indicates that these materials are complex and have multiple retardation times.

Results of the monotonic test are given in Table 2 and Figure 7. The apparent elastic modulus, defined as the slope of the linear portion of apparent stress-strain curve, and flexural strength obtained from the monotonic tests on AIDBD and NR samples are presented in Table 2. Dry apparent elastic moduli were found to be $2.84(\pm 0.47)$ GPa and $2.68(\pm 0.20)$ GPa for AIDBD-1 and NR-1, respectively. For the formulation-2 in dry environment, AIDBD and NR samples have apparent elastic moduli of $2.50(\pm 0.31)$ GPa and $2.67(\pm 0.20)$ GPa, respectively. When AIDBD and NR samples were tested under wet saturated environment, apparent elastic moduli are reduced compared to that of dry conditions. For AIDBD-1, AIDBD-2, NR-1 and NR-2 apparent elastic moduli was found to be $0.90(\pm 0.30)$, $0.50(\pm 0.31)$, $1.27(\pm 0.16)$ and $0.88(\pm 0.2)$ GPa respectively in wet condition. Elastic modulus for demineralized bovine dentin(DBD) was found to be $41.56(\pm 4.30)$ MPa in wet state.

The flexural strength obtained from the monotonic tests is also given in Table 2. It was found to be $140(\pm 13)$ MPa and $138(\pm 5)$ MPa in dry, and $38(\pm 2)$ MPa and $17(\pm 2)$ MPa in wet conditions for the AIDBD-1 and AIDBD-2, respectively. The flexural strength for the NR-1 and NR-2 samples was $100(\pm 3)$ MPa and $104(\pm 9)$ MPa, respectively in dry conditions, and $42(\pm 6)$ MPa and $26(\pm 2)$ MPa, respectively in wet conditions.

3.4 Evaluation of Viscoelastic Model

To identify the creep compliance parameters J_0, J_1, J_2, J_3, J_4 for AIDBD and NR samples, creep data from the experiments was fitted with Eq(2) using a non-linear least-square

subroutine from Matlab under the constraint that the creep constants are non-negative^{32,33}. The calculated model parameters along with the goodness of fit R^2 are given in Table 3. The frequency dependent storage modulus, loss modulus and $\tan(\delta)$ calculated from creep compliance data using Eq(4) are shown in Figure 8. The values of storage, loss and $\tan(\delta)$ at the frequency of 0.1Hz, which is in the range of cited frequency during mastication^{34–36}, for AIDBD and NR are given in Table 4. Storage moduli for AIDBD-1 and AIDBD-2 in dry and wet conditions were found to be 1.94 and 2.0GPa and 0.7 and 0.5GPa, respectively. Relaxation function $G(t)$ is also obtained from the creep compliance data. The calculated relaxation modulus parameters G_0, G_1, G_2, G_3, G_4 and relaxation times $\tau_1, \tau_2, \tau_3, \tau_4$ are given in Table 5 for AIDBD and NR. Stress relaxation response for AIDBD and NR at 1% applied strain is given in Figure 9. Under the wet environment, stress relaxes to a constant value for both AIDBD and NR in 1400 minute but, stress continues to decrease with time for both AIDBD and NR in the dry condition. Further we have also used the relaxation function $G(t)$ with Eq(5) to predict rate dependent elastic modulus. To be consistent with experimental data, strain was chosen to be 0.0036/min, which corresponds to 60 $\mu\text{m}/\text{min}$ displacement rate in 3 point bending. The comparison of the predicted elastic modulus using the viscoelastic model and from monotonic experiments is given in Figure 10.

4. Discussion

Under dry conditions, the creep response for NR and AIDBD samples is similar for both formulations. In contrast, the creep curves for AIDBD samples stored and tested in water, show instantaneous strain almost ~ 3 and ~ 4 times of the dry case for formulations 1 and 2 respectively. This increase in instantaneous strain indicates plasticization of AIDBD due to storage in water. Similar results were also obtained for NR which are in the agreement with our previous work¹⁹. We also find that as compared to formulation-1, both the wet AIDBD and NR samples of formulation-2 have significantly larger deformation under creep loading. This difference is due to the relatively hydrophilic BMPB²⁸ in formulation-2, which increases the overall hydrophilicity resulting in a higher creep strain under applied stress. We note that in all the creep curves, the primary creep is dominant and the creep deformation appears to reach asymptotic value, indicating that the creep behavior under the low applied load can be treated as linear viscoelastic. This observation is confirmed by the excellent goodness-of-fit of the observed data with the linear 4-element generalized Kelvin-Voigt model. Further, it is interesting to observe that the 4-element model is necessary which suggests that both AIDBD and NR are complex materials with more than one characteristic retardation or relaxation times. The predicted storage moduli, based upon the fitted creep compliances, show an increase with frequency and appear to reach an asymptote at frequency of 0.1 Hz for AIDBD and NR in both dry and wet conditions. Compared to dry state, the storage moduli are significantly smaller under wet conditions. The predicted loss moduli in dry condition showed two peaks at 0.0003 and 0.02Hz. In contrast, the predicted loss moduli under wet conditions show a complex behavior with frequency including multiple peaks or saddles. The predicted $\tan(\delta)$ was found to have a similar trend as that of loss modulus with well-defined peak for the dry case and a complex trend for the wet case. We note that the fitted model appears to capture the behavior of the investigated materials both in dry and wet conditions as shown by the reasonable agreement of the predicted and

the measured rate dependent elastic moduli shown in Figure 10. It should be noted however that, the predicted elastic moduli using the fitted linear viscoelastic model is sensitive to initial strain in creep data. A small variation can cause relatively significant change in the predicted elastic modulus. In this work, relatively small sample size $n=3$ was used, which for testing under dry condition results in larger standard deviation due to relatively smaller signal-to-noise ratio for small strain amplitudes. Therefore, the predictions for dry samples are not within the standard of deviation of measured values, although the trends are captured well by the model. Clearly, the advantage of viscoelastic modeling is that using a simple creep experiment we can obtain other properties such as storage and loss moduli as function of frequency, elastic moduli at different rates and stress relaxation behavior at different strain level. It is important to obtain all of these properties to understand the complete mechanical response of AIDBD (or collagen-adhesive composites) and the NR (or neat resin) samples. To obtain all of the above mentioned properties using lab experiments is both time consuming and expensive. Therefore prediction of viscoelastic properties using relatively simple creep experiment data is an attractive alternative to conventional mechanical tests.

From the results of the monotonic tests we found that apparent elastic moduli of NR and AIDBD in dry condition were not significantly different from each other. However, the flexural strengths of both AIDBD samples are significantly higher compared to their NR counterpart in the dry condition. This is due to the presence of demineralized bovine collagen in AIDBD samples which provides a fiber network that acts as reinforcement under the applied load. As a result, AIDBD samples fail at higher magnitudes of stress and strain. In NR beam samples this type of fiber network is absent and the sample failure is not impeded by mechanisms such as fiber bridging. Consequently, we found that AIDBD samples have higher toughness when tested in dry environment. In contrast, when AIDBD sample is stored in water for 5 days and tested in water, the apparent elastic moduli decreases significantly. Similar softening is found for NR samples, however, in comparison, the AIDBD samples suffer a considerably greater softening. The softening of the NR polymers upon water exposure is attributable to plasticization, which leads to less constrained movement of the polymer chains and collagen fibers since part of the molecular scale interactions are disrupted by water. Furthermore, the wet AIDBD-2 samples suffer greater effect of plasticization due to the hydrophilicity of the polymer and generally have lower flexural strength. For both adhesive formulations, the presence of collagen seems to be a controlling factor for AIDBD samples. A simple volume averaging to estimate the elastic moduli for AIDBD in the wet environment gives ~ 0.6 GPa and 0.4 GPa for formulation 1 and 2, respectively, which is similar to that measured. However, the behavior at larger strain appears to deviate considerably from the simple volume average. We believe that not only the collagen softens considerably as seen from Figure 7(b), but the interactions of the dentin adhesive and collagen must experience significant disruption due to water.

Finally, it is worth commenting that relatively few previous studies have been conducted to obtain the mechanical properties of resin infiltrated dentin. Yasuda et al^{25,26} obtained the elastic moduli of adhesive infiltrated dentin samples using ultrasonic testing. They have reported the values of elastic moduli for their adhesive infiltrated dentin to be higher than

that of the neat adhesive. These ultrasonic experiments were performed for saturated samples at high frequencies (5–10 MHz). Under these high frequencies a typically stiffer response is obtained for water saturated materials owing to the inability of unbound water to migrate under loading, leading to undrained conditions^{21,37}. Also a dimensional analysis of their expression for elastic modulus appears to indicate some inconsistency. Therefore the values reported by Yasuda et al cannot be directly compared to the elastic modulus obtained from our experiments. Recently Ryou et al²⁴ performed nanomechanical studies to characterize resin-infiltrated dentin. These nanomechanical tests were performed at very small indentation depth <10nm at frequency of 100Hz and reported a value of 3.5(±0.3) GPa for adhesive infiltrated dentin and 2.7(±0.3) GPa for neat adhesive under hydrated condition with uncharacteristically small standard deviations. The nanomechanical tests interrogate very small volumes, therefore the properties obtained from these nanomechanical tests cannot be considered as the true representation of bulk properties obtained from the conventional mechanical tests used in this study. In a study measuring bulk properties under quasi-static conditions, Chiaraputt et al²² performed 3 point bending tests and reported that for saturated wet environment, the elastic moduli of resin infiltrated dentin is lower than its neat resin counterpart, which agrees with our experimental findings. Similarly Gu et al²³ also reported lower elastic moduli for resin infiltrated dentin compared to neat resin using simple volume averaging. It is clear, that these few contradictory experimental efforts have only examined a subset of mechanical behavior and none appears to have investigated creep and rate-dependent behavior in the depth performed herein.

The results presented in this paper show that the mechanical behavior of even ideal collagen adhesive composites, termed here as adhesive infiltrated demineralized bovine dentin, depends upon a number of factors, such as (a) the moisture conditions, (b) dentin adhesive characteristics, (c) the relative proportions of dentin adhesive and collagen, (d) the loading level, and (e) the loading rate. The collagen-adhesive composite formed in clinical conditions is much more complex than the adhesive-collagen composite investigated here. In the clinical environment dentin adhesive only partially infiltrates demineralized dentin and undergoes phase separation^{21,27,38}. The extent of adhesive penetration at the a-d interface was studied by Wang and Spencer³⁹. The hydrophilic adhesive components (including HEMA) diffuse more readily into the demineralized dentin zone than the relatively hydrophobic BisGMA. The resulting adhesive phased polymerized in the presence of water can have complex mechanical behavior²¹.

In contrast to the clinical setting, the AIDBD specimens used in this study were produced under controlled laboratory conditions resulting in complete infiltration of demineralized dentin. Furthermore, the dentin demineralization is highly heterogeneous^{40,41} and the dentin composition at the scales at which a-d interface forms can be profoundly affected by caries^{42,43}. In addition, the dentin adhesives used under clinical conditions may also be composed of different co-monomer systems as well as various solvents.

It is noteworthy that the adhesive-collagen composite represents only one component of the complex material-structural construct formed at the a-d interface. In our previous work we have reported through finite element simulations how the load is transferred at the a-d interface and how its fatigue behavior and durability is affected by the material components

and microstructure of this complex construct¹¹⁻¹³. We have also shown that the mechanical properties of dentin adhesive are affected by the moisture conditions, loading rate and loading-level^{18,19}. The non-linear, moisture and rate-dependent behavior requires new physics-based mathematical model to describe the behavior of adhesive and adhesive-collagen composites in a comprehensive manner^{21,43}. To this end, the study reported here forms part of a larger effort to understand a-d interface through a combination of mathematical modeling and experimental characterization.

5. Summary and Conclusions

Ideal collagen-adhesive composites formed by the infiltration of dentin adhesives into demineralized bovine dentin was investigated for their time and rate dependent behavior under conditions that simulate the wet functional environment found in the oral cavity. To study the effect of adhesive hydrophilicity on the properties of composites two types of dentin adhesives of different hydrophilicity were used. Creep and monotonic tests were performed on rectangular beam samples in 3 point bending configuration under dry and wet conditions. The monotonic test results showed that collagen-adhesive composites samples have similar elastic modulus, however higher modulus of toughness than neat adhesive in dry conditions. Whereas, under wet condition both the elastic modulus and the strength of collagen-adhesive composites decrease compared to that of neat adhesives. The results of the creep tests under small stress amplitude showed that for both the collagen-adhesive composites and the neat resins, the behavior is linear viscoelastic in dry and wet environment. Creep and rate-dependent behavior of such composites have been rarely examined and the current literature information on their mechanical properties contains contradictory results.

To capture the creep response, a linear 4-element generalized Kelvin-Voigt model was required, indicating that the adhesive-collagen composites are complex materials with several characteristics time-scales whose mechanical behavior will be significantly affected by loading rates and frequencies even under small amplitudes. The developed model was used to predict frequency-dependent and rate-dependent properties of collagen-adhesive composites and neat resin samples. The model was shown to perform satisfactorily for linear behavior. However, at higher stress-levels and under transient moisture condition we expect the creep behavior to be highly nonlinear, which will require enhanced models for describing the behavior as well as further creep testing at higher stress-levels and monotonic testing at different loading rates.

Finally we note that these materials form a part of the adhesive-dentin interface, which is a thin complex construct of several material components extending over the cavity surface of a complicated geometrical shape. The overall behavior of the restoration is, therefore, not only affected by adhesive-collagen composites, but also by its interactions with the other material components, as well as the overall mastication loading. A systematic study is needed to determine how these materials impact the overall performance of the restoration. However, it is clear from the findings of this paper that these materials represent a weak link.

ACKNOWLEDGMENTS

The authors gratefully acknowledge financial support for this project by National Institutes of Health/National Institute of Dental and Craniofacial Research (R01DE014392, 3R01DE014392-08S1, and R01 DE022054).

References

1. Reece TB, Maxey TS, Kron IL. A prospectus on tissue adhesives. *The American journal of surgery*. 2001; 182(2):S40–S44.
2. Singer AJ, Thode HC Jr. A review of the literature on octylcyanoacrylate tissue adhesive. *The American journal of surgery*. 2004; 187(2):238–248.
3. Drury JL, Mooney DJ. Hydrogels for tissue engineering: scaffold design variables and applications. *Biomaterials*. 2003; 24(24):4337–4351. [PubMed: 12922147]
4. Shanmugasundaram N, Ravichandran P, Reddy PN, Ramamurthy N, Pal S, Rao KP. Collagen-chitosan polymeric scaffolds for the in vitro culture of human epidermoid carcinoma cells. *Biomaterials*. 2001; 22(14):1943–1951. [PubMed: 11426872]
5. Tang SQ, Yang W, Mao X. Agarose/collagen composite scaffold as an anti-adhesive sheet. *Biomedical Materials*. 2007; 2(3):S129–S134. [PubMed: 18458457]
6. Spencer P, Ye Q, Park J, Topp EM, Misra A, Marangos O, Wang Y, Bohaty BS, Singh V, Sene F, et al. Adhesive/Dentin interface: the weak link in the composite restoration. *Annals of Biomedical Engineering*. 2010; 38(6):1989–2003. [PubMed: 20195761]
7. Pashley DH, Ciucchi B, Sano H, Horner JA. Permeability of dentin to adhesive agents. *Quintessence Int*. 1993; 24(9):618–631. [PubMed: 8272500]
8. Spencer P, Ye Q, Misra A, Bohaty BS, Singh V, Parthasarathy R, Sene F, Goncalves SEDP, Laurence J. Durable bonds at the adhesive/dentin interface: an impossible mission or simply a moving target? *Braz Dent Sci*. 2012; 15(1):4–18. [PubMed: 24855586]
9. Kleverlaan CJ, Feilzer AJ. Polymerization shrinkage and contraction stress of dental resin composites. *Dent Mater*. 2005; 21(12):1150–1157. [PubMed: 16040118]
10. Roulet JF. Benefits and Disadvantages of Tooth-coloured Alternatives to Amalgam. *J Dent. J Dent*. 1997; 25:459–473.
11. Misra A, Spencer P, Marangos O, Wang Y, Katz JL. Micromechanical Analysis of Dentin/Adhesive Interface by the Finite Element Method. *J Biomed Mater Res Part B: Appl Biomater*. 2004; 70B:56–65. [PubMed: 15199584]
12. Misra A, Spencer P, Marangos O, Wang Y, Katz JL. Parametric Study of the Effect of Phase Anisotropy on the Micromechanical Behavior of dentin-adhesive Interface. *Journal of Royal Society Interface*. 2005; 2:145–157.
13. Singh V, Misra A, Marangos O, Park J, Ye Q, Kieweg SL, Spencer P. Fatigue life prediction of dentin–adhesive interface using micromechanical stress analysis. *Dental Materials*. 2011; 27(9):e187–e195. [PubMed: 21700326]
14. Armstrong S, Geraldeli S, Maia R, Raposo LH, Soares CJ, Yamagawa J. Adhesion to tooth structure: a critical review of "micro" bond strength test methods. *Dent Mater*. 2010; 26(2):e50–e62. [PubMed: 20045179]
15. Armstrong SR, Boyer DB, Keller JC. Microtensile bond strength testing and failure analysis of two dentin adhesives. *Dental Materials*. 1998; 14(1):44–50. [PubMed: 9972150]
16. Roeder L, Pereira PN, Yamamoto T, Ilie N, Armstrong S, Ferracane J. Spotlight on bond strength testing—unraveling the complexities. *Dent Mater*. 2011; 27(12):1197–1203. [PubMed: 21944280]
17. Yiu CKY, King NM, Pashley DH, Suh BI, Carvalho RM, Carrilho MRO, Tay FR. Effect of resin hydrophilicity and water storage on resin strength. *Biomaterials*. 2004; 25(26):5789–5796. [PubMed: 15147825]
18. Singh V, Misra A, Marangos O, Park J, Ye Q, Kieweg SL, Spencer P. Viscoelastic and fatigue properties of model methacrylate-based dentin adhesives. *J Biomed Mater Res B Appl Biomater*. 2010; 95(2):283–290. [PubMed: 20848661]

19. Singh V, Misra A, Parthasarathy R, Ye Q, Park J, Spencer P. Mechanical properties of methacrylate-based model dentin adhesives: Effect of loading rate and moisture exposure. *J Biomed Mater Res B Appl Biomater*. 2013
20. Parthasarathy R, Misra A, Park J, Ye Q, Spencer P. Diffusion coefficients of water and leachables in methacrylate-based crosslinked polymers using absorption experiments. *J Mater Sci Mater Med*. 2012; 23(5):1157–1172. [PubMed: 22430592]
21. Misra A, Parthasarathy R, Ye Q, Singh V, Spencer P. Swelling equilibrium of dentin adhesive polymer formed on the water adhesive phase boundary: Experiments and micromechanical model. *Acta Biomaterialia*. 2014; 10:330–342. [PubMed: 24076070]
22. Chiaraputt S, Mai S, Huffman BP, Kapur R, Agee KA, Yiu CK, Chan DC, Harnirattisai C, Arola DD, Rueggeberg FA, et al. Changes in resin-infiltrated dentin stiffness after water storage. *J Dent Res*. 2008; 87(7):655–660. [PubMed: 18573986]
23. Gu LS, Huffman BP, Arola DD, Kim YK, Mai S, Elsalanty ME, Ling JQ, Pashley DH, Tay FR. Changes in stiffness of resin-infiltrated demineralized dentin after remineralization by a bottom-up biomimetic approach. *Acta Biomater*. 2010; 6(4):1453–1461. [PubMed: 19887126]
24. Ryou H, Pashley DH, Tay FR, Arola D. A characterization of the mechanical behavior of resin-infiltrated dentin using nanoscopic Dynamic Mechanical Analysis. *Dent Mater*. 2013; 29(7):719–728. [PubMed: 23639453]
25. Yasuda G, Inage H, Kawamoto R, Shimamura Y, Takubo C, Tamura Y, Koga K, Miyazaki M. Changes in elastic modulus of adhesive and adhesive-infiltrated dentin during storage in water. *J Oral Sci*. 2008; 50(4):481–486. [PubMed: 19106478]
26. Yasuda G, Inage H, Takamizawa T, Kurokawa H, Rikuta A, Miyazaki M. Determination of elastic modulus of demineralized resin-infiltrated dentin by self-etch adhesives. *Eur J Oral Sci*. 2007; 115(1):87–91. [PubMed: 17305722]
27. Wang Y, Spencer P. Hybridization efficiency of the adhesive/dentin interface with wet bonding. *J Dent Res*. 2003; 82(2):141–145. [PubMed: 12562889]
28. Park J, Ye Q, Singh V, Kieweg SL, Misra A, Spencer P. Synthesis and evaluation of novel dental monomer with branched aromatic carboxylic acid group. *J Biomed Mater Res B Appl Biomater*. 2011
29. Park JG, Ye Q, Topp EM, Misra A, Spencer P. Water Sorption and Dynamic Mechanical Properties of Dentin Adhesives with a Urethane-Based Multifunctional Methacrylate Monomer. *Dental Materials*. 2009; 25:1569–1575. [PubMed: 19709724]
30. Lakes, RS. *Viscoelastic solids*. Boca Raton: CRC Press; 1999. p. 476
31. Wineman, AS.; Rajagopal, KR. *Mechanical response of polymers : an introduction*. Cambridge, England New York: Cambridge University Press; 2000. p. x317
32. Chen, T. *Determining a Prony Series for a Viscoelastic Material from Time Varying Strain Data*. U.S Army Research Laboratory; 2000.
33. Dooling PJ, Buckley CP, Hinduja S. An Intermediate Model Method for Obtaining a Discrete Relaxation Spectrum from Creep Data. *Rheological Acta*. 1997; 36:472–482.
34. Walker MP, Teitelbaum HK, Eick JD, Williams KB. Effects of simulated functional loading conditions on dentin, composite and laminate structures. *J Biomed Mater Res B Appl Biomater*. 2009; 88(2):492–501. [PubMed: 18823019]
35. Po JMC, Kieser JA, Gallo LM, Tesenyi AJ, Herbison P, Farella M. Time-Frequency Analysis of Chewing Activity in the Natural Environment. *Journal of Dental Research*. 2011; 90(10):1206–1210. [PubMed: 21810620]
36. Nalla RK, Imbeni V, Kinney JH, Staninec M, Marshall SJ, Ritchie RO. In Vitro Fatigue Behavior of Human Dentin with Implications for Life Prediction. *Journal of Biomedical Material Research*. 2003; 66A:10–20.
37. Misra, A.; Marangos, O.; Parthasarathy, R.; Spencer, P. Micro-scale analysis of compositional and mechanical properties of dentin using homotopic measurements. In: Andraeus, U.; Iacoviello, D., editors. *Biomedical Imaging and Computational Modeling in Biomechanics*. Netherlands: Springer; 2013. p. 131-141.
38. Spencer P, Wang Y. Adhesive phase separation at the dentin interface under wet bonding conditions. *Journal of Biomedical Materials Research*. 2002; 62(3):447–456. [PubMed: 12209931]

39. Wang Y, Spencer P. Quantifying adhesive penetration in adhesive/dentin interface using confocal Raman microspectroscopy. *J Biomed Mater Res.* 2002; 59(1):46–55. [PubMed: 11745536]
40. Marangos O, Misra A, Spencer P, Katz JL. Scanning acoustic microscopy investigation of frequency-dependent reflectance of acid- etched human dentin using homotopic measurements. *IEEE Trans Ultrason Ferroelectr Freq Control.* 2011; 58(3):585–595. [PubMed: 21429849]
41. Wieliczka DM, Spencer P, Kruger MB. Raman mapping of the dentin/adhesive interface. *Appl. Spectrosc.* 1996; 50:1500–1504.
42. Marangos O, Misra A, Spencer P, Bohaty B, Katz JL. Physico-mechanical properties determination using microscale homotopic measurements: Application to sound and caries-affected primary tooth dentin. *Acta Biomaterialia.* 2009; 5(4):1338–1348. [PubMed: 19059013]
43. Misra A, Singh V. Micromechanical model for viscoelastic materials undergoing damage. *Continuum Mechanics and Thermodynamics.* 2013; 25(2–4):343–358.

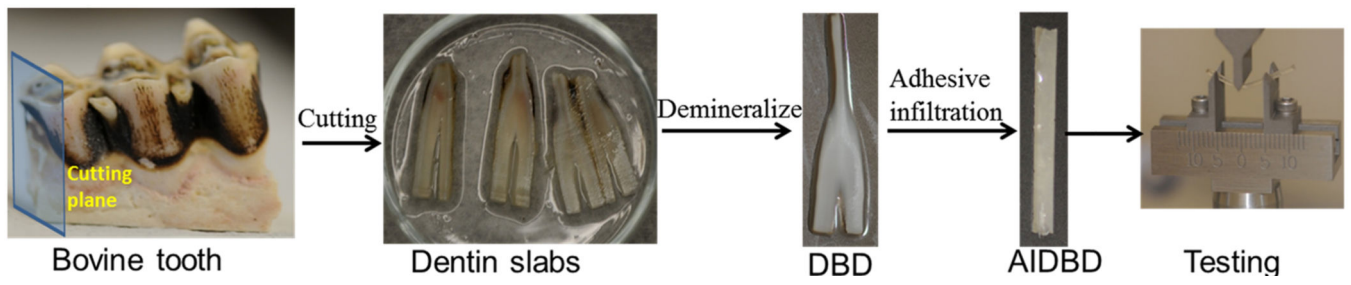


Figure 1.
Steps involved in obtaining AIDBD samples

Author Manuscript

Author Manuscript

Author Manuscript

Author Manuscript

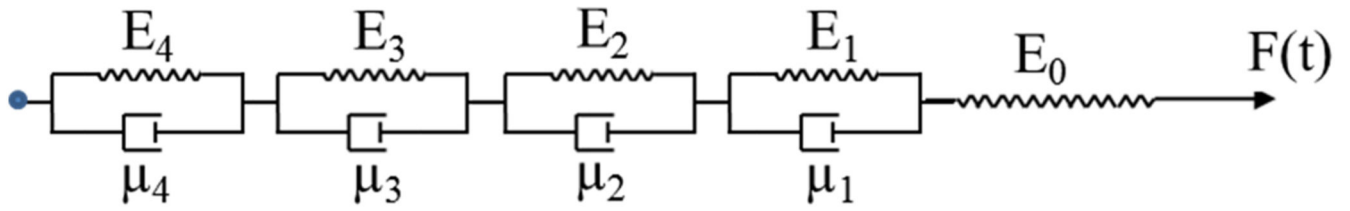


Figure 2.
Generalized Kelvin-Voigt model with 4 elements.

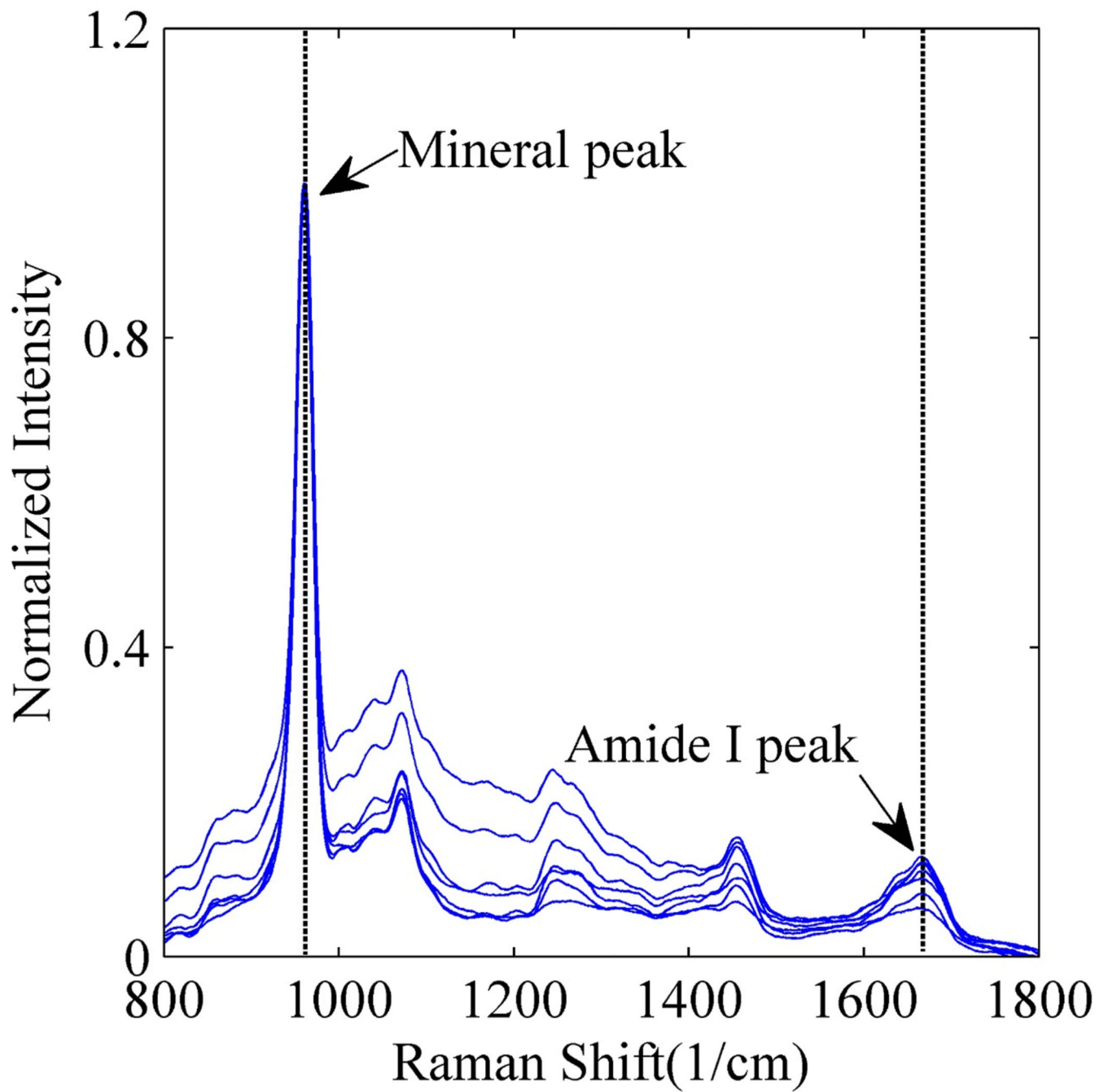


Figure 3.
Raman spectra of bovine dentin acquired at different locations before demineralization process.

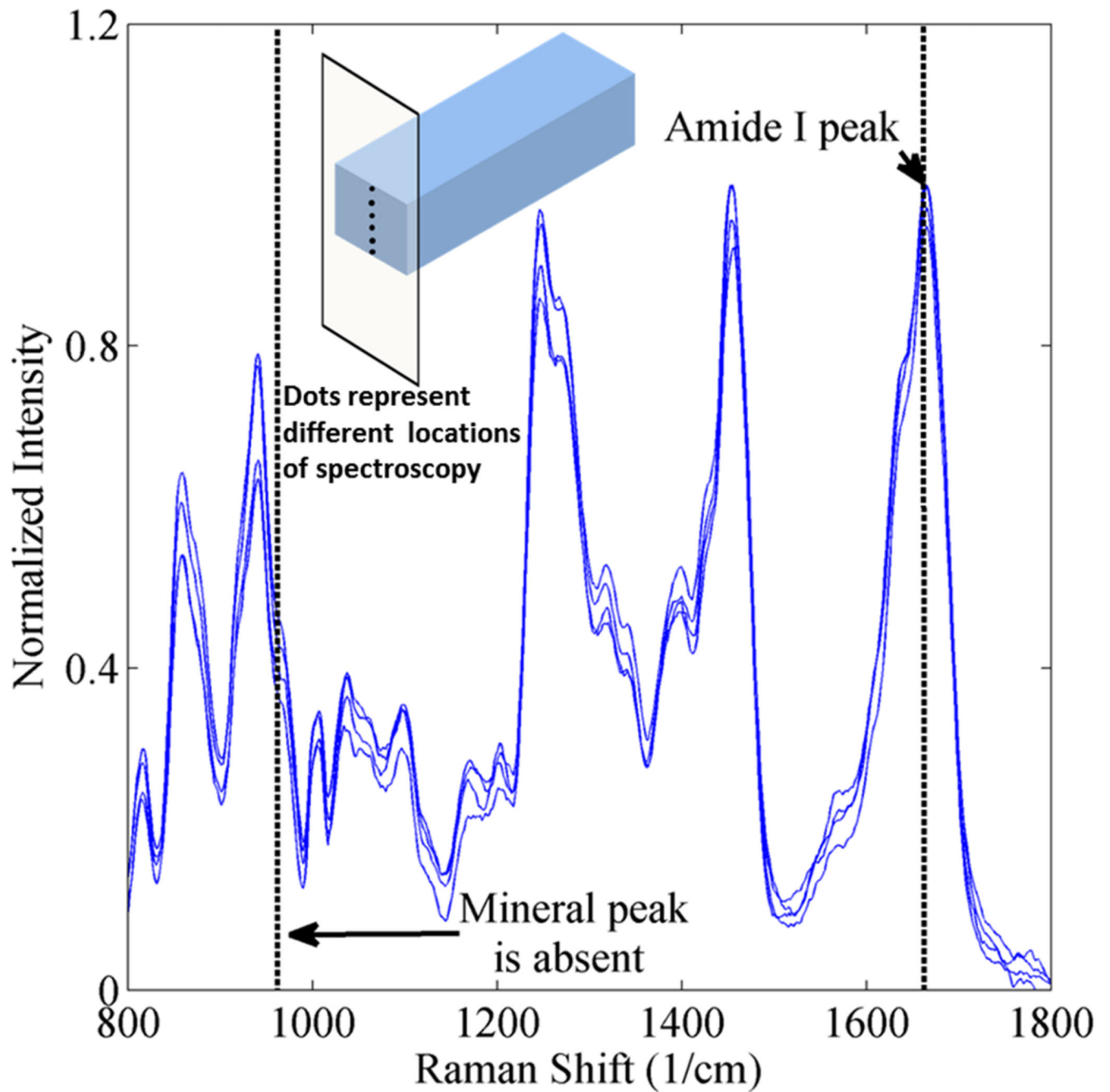


Figure 4. Raman spectra of bovine dentin after the demineralization process acquired along the thickness for one randomly selected sacrificial sample as shown in the inset.

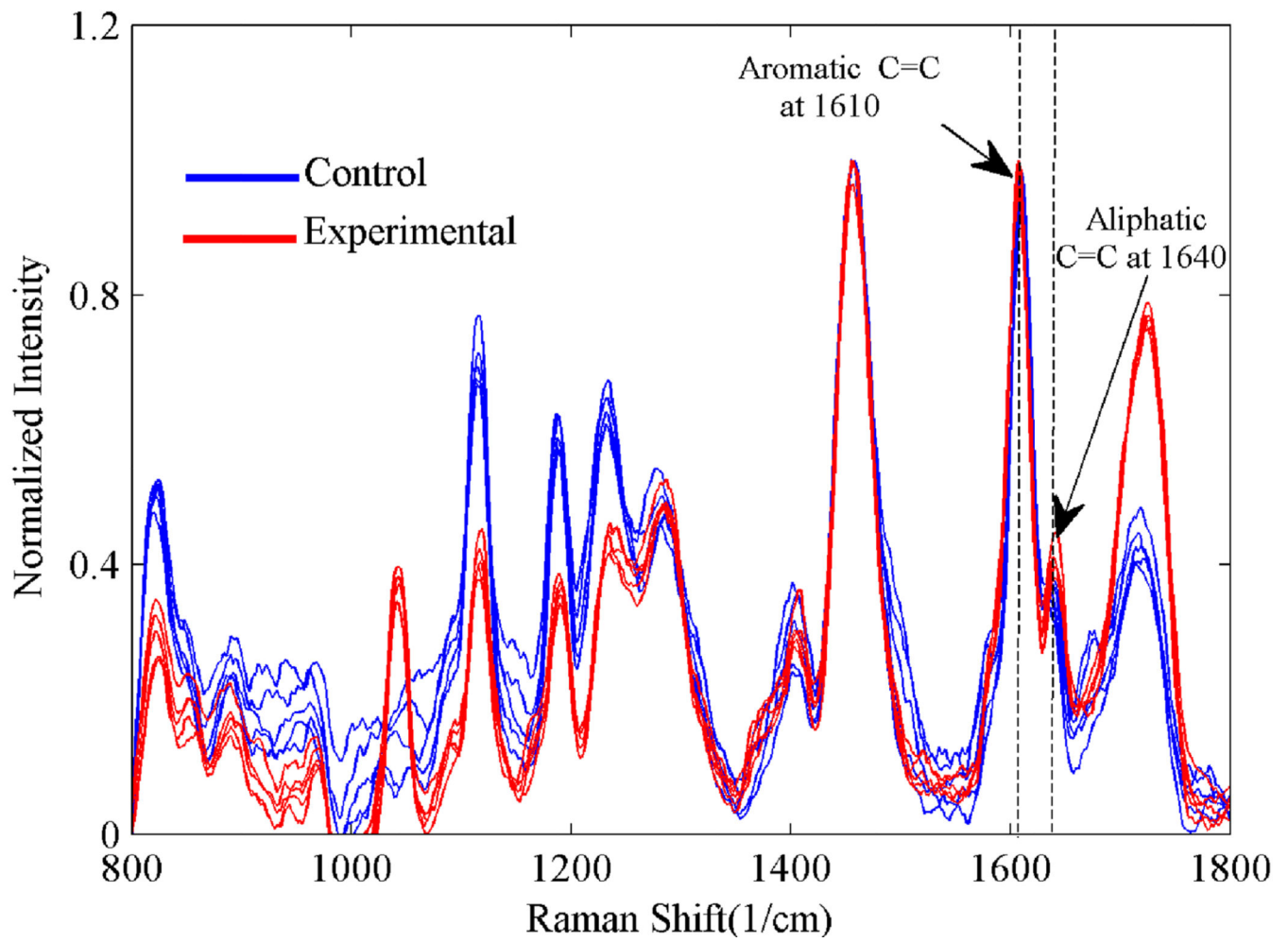


Figure 5.

To check for complete infiltration of dentin adhesive into DBD, Raman spectra were acquired from points across the cross-section of one randomly selected sacrificial AIDBD samples as shown in the inset of Figure 4.

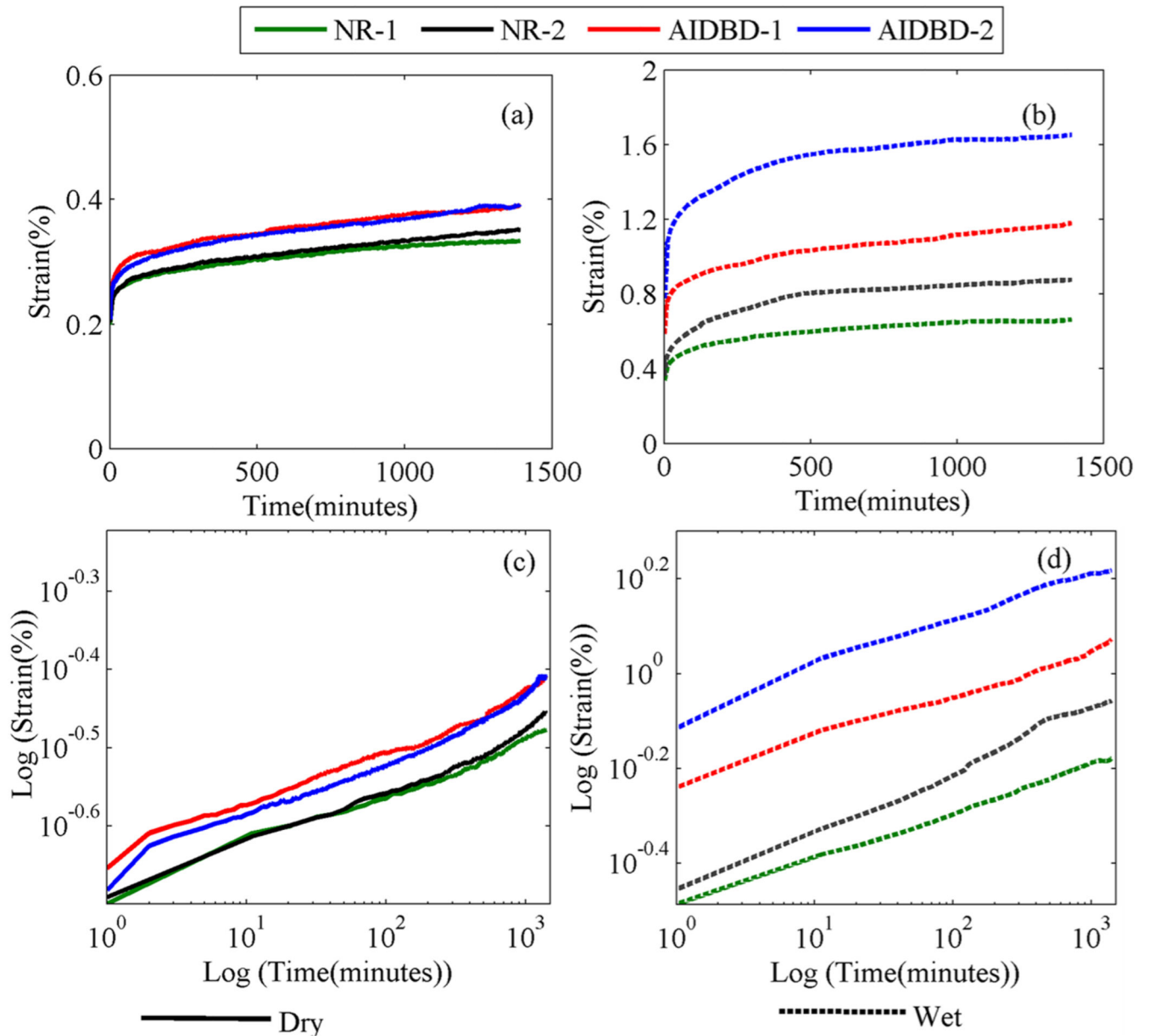


Figure 6.

Apparent creep curves for AIDBD or hybrid layer mimics and the neat resins (NR) at stress amplitude of 4.5MPa, (a) dry condition, and (b) wet saturated environment. Plots (c) and (d) represent the creep data in log-log scales in dry and wet conditions respectively.

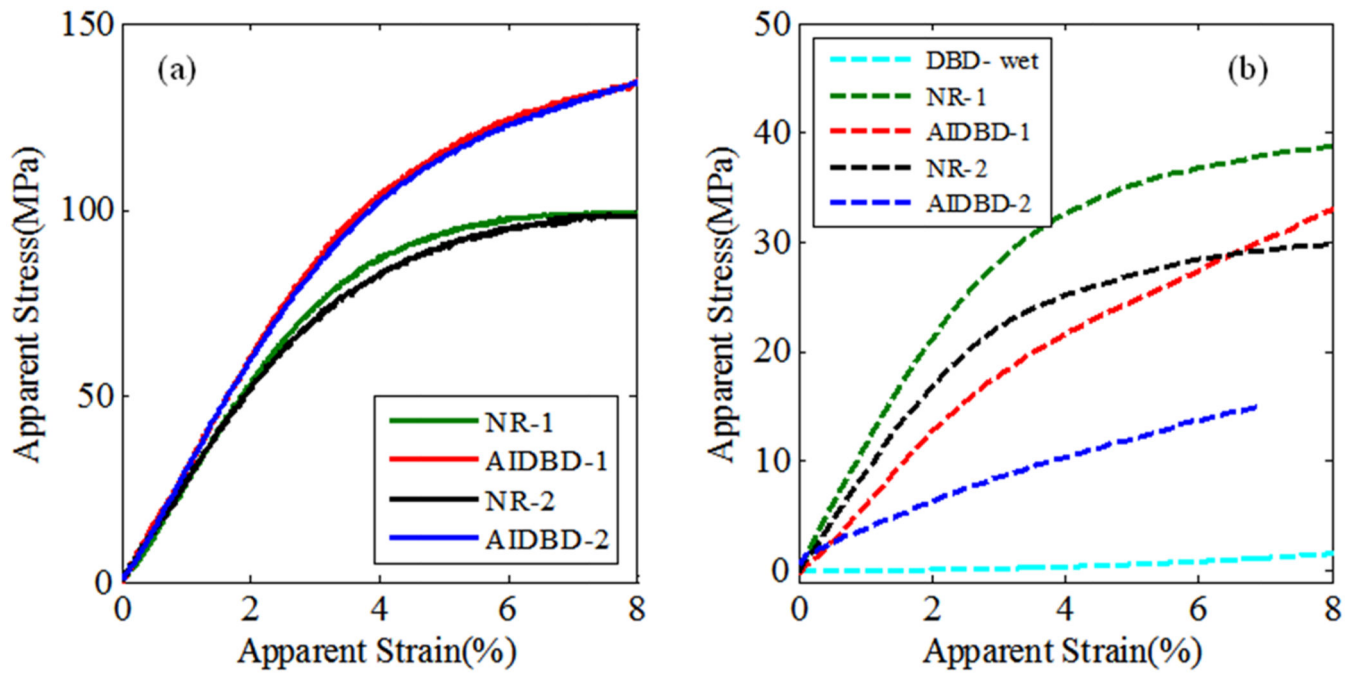


Figure 7. Apparent stress-strain curves for AIDBD or hybrid layer mimics and the neat resins (NR) under monotonic loading: (a) under dry condition and (b) under wet saturated condition.

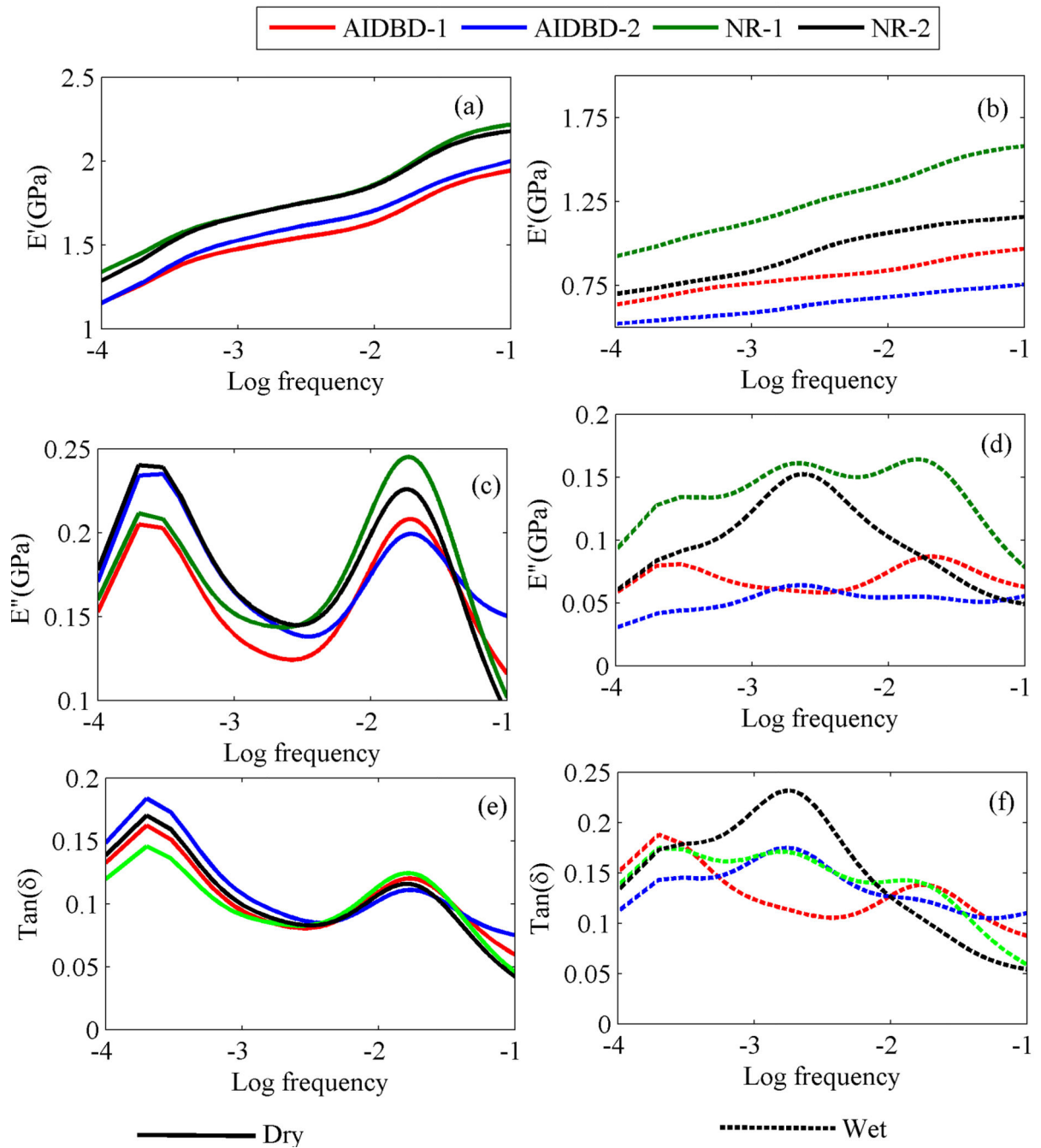


Figure 8. Predicted storage and loss moduli and $\tan(\delta)$ at different frequencies (in Hz) for AIDBD and neat resins(NR) (a) dry storage modulus, (b) wet storage modulus, (c) dry loss modulus, (d) wet loss modulus, (e) dry $\tan\delta$, and (f) wet $\tan\delta$.

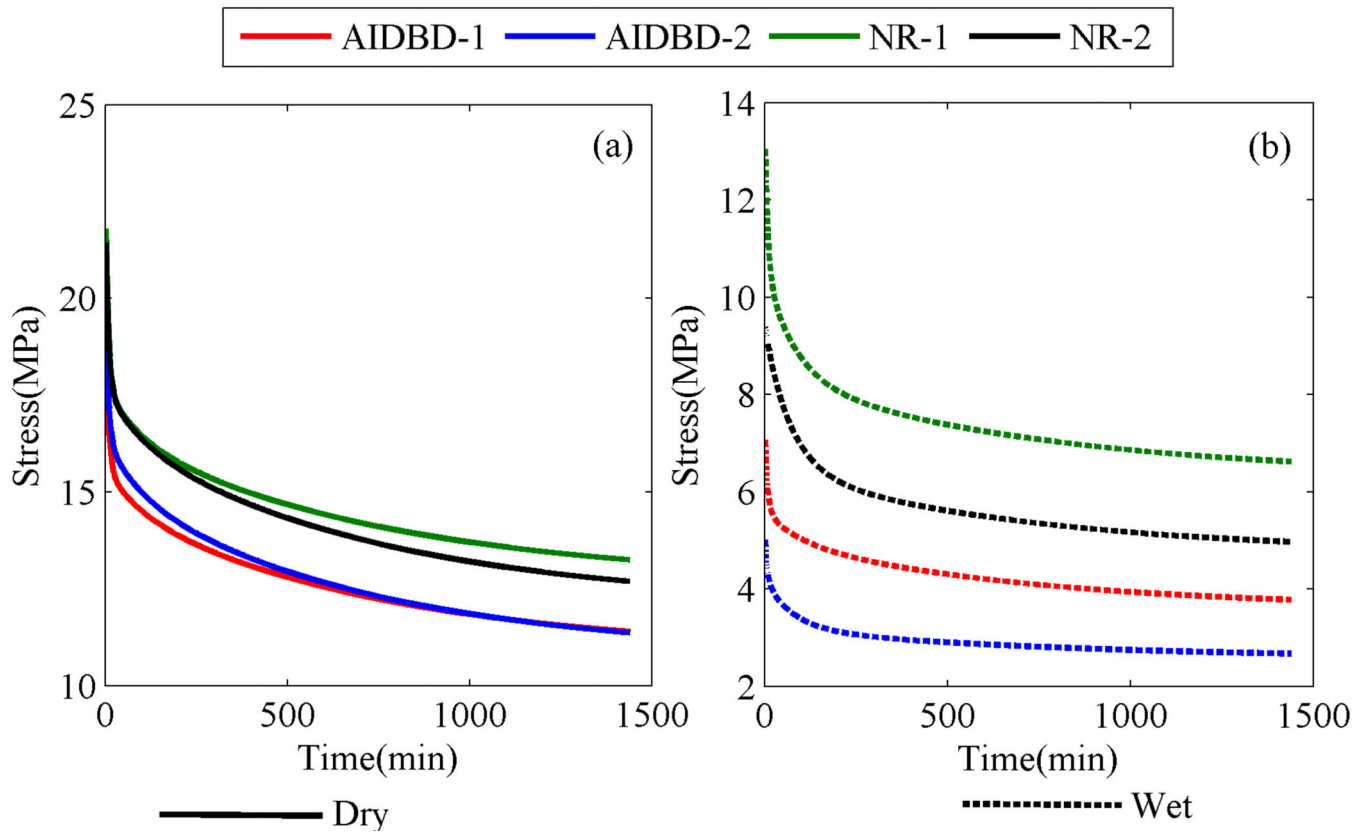


Figure 9. Predicted stress relaxation behavior at strain amplitude of $\varepsilon_{11}=0.01$, for AIDBD and neat resin (NR) sample (a) in dry and (b) wet environments.

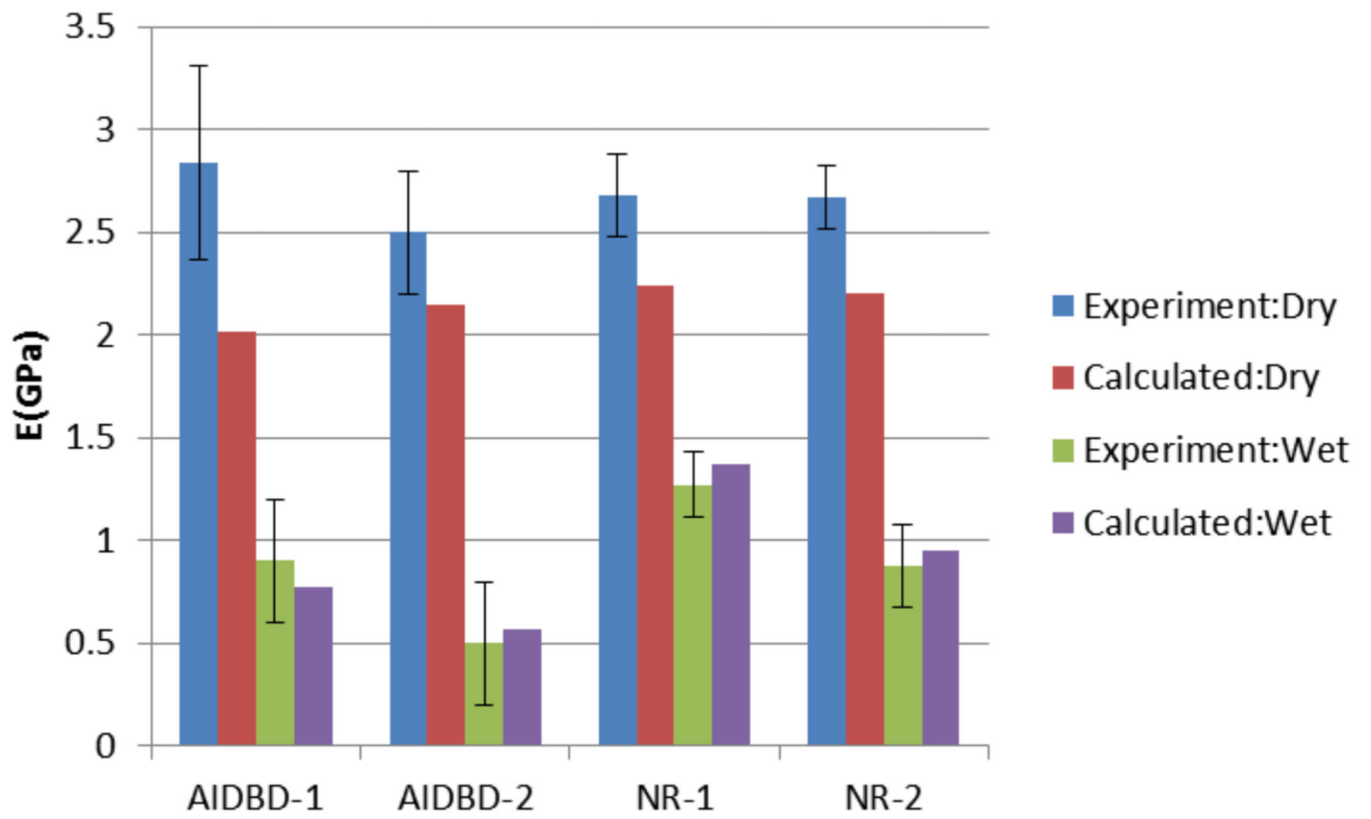


Figure 10. Comparison of predicted and calculated elastic moduli for AIDBD and neat resin (NR) sample in dry and wet environment.

Table 1

Weight fractions, volume fractions for AIDBD samples in saturated state

	Control	
	Weight fraction (%)	Volume fraction (%)
Adhesive	45.43(\pm 1.15)	42.12(\pm 1.10)
DBD	39.78(\pm 1.62)	43.33(\pm 1.14)

Author Manuscript

Author Manuscript

Author Manuscript

Author Manuscript

Table 2

Apparent elastic modulus E(GPa) and flexural strength f(MPa) for AIDBD and neat resin

	AIDBD-1		AIDBD-2		NR-1		NR-2	
	Dry	Wet	Dry	Wet	Dry	Wet	Dry	Wet
E(GPa)	2.84(±0.47)	0.90(±0.30)	2.50(±0.30)	0.50(±0.31)	2.68(±0.20)	1.27(±0.16)	2.67(±0.020)	0.88(±0.20)
f(MPa)	140(±13)	38(±2)	139(5)	17(±2)	100(±3)	42(±6)	104(±9)	26(±2)

Table 3 Creep compliance parameters for AIDBD and NR obtained using nonlinear least square fitting.

Parameters I/GPa	AIDBD-1		AIDBD-2		NR-1		NR-2	
	Dry	Wet	Dry	Wet	Dry	Wet	Dry	Wet
J_0	0.493	1.278	0.462	1.706	0.445	0.726	0.452	1.045
J_1	0.024	0.136	0.046	0.340	0.005	0.027	0.004	0.070
J_2	0.121	0.360	0.100	0.320	0.113	0.176	0.105	0.115
J_3	0.040	0.195	0.047	0.723	0.040	0.243	0.038	0.564
J_4	0.243	0.820	0.272	0.803	0.188	0.410	0.228	0.566
Goodness of fit- R^2	0.995	0.994	0.990	0.987	0.985	0.990	0.979	0.984

Table 4

Storage, Loss and Tan(δ) at 0.1Hz frequency obtained from viscoelastic model

Parameters	AIDBD-1		AIDBD-2		NR-1		NR-2	
	Dry	Wet	Dry	Wet	Dry	Wet	Dry	Wet
Storage(GPa)	1.94	0.7	2.00	0.50	2.21	1.33	2.21	0.90
Loss(MPa)	116	62.67	150.20	55.56.	101.85	78.36	91.75	49.15
Tan(δ)	0.06	0.087	0.075	0.11	0.046	0.06	0.042	0.055

Table 5
Stress relaxation modulus parameters and relaxation times for AIDBD and NR obtain from creep compliance data.

Parameters GPa	AIDBD-1		AIDBD-2		NR-1		NR-2	
	Dry	Wet	Dry	Wet	Dry	Wet	Dry	Wet
G ₀	1.086	0.360	1.080	0.257	1.266	0.632	1.207	0.473
G ₁	0.100	0.080	0.204	0.101	0.027	0.053	0.023	0.009
G ₂	0.370	0.142	0.322	0.067	0.456	0.263	0.415	0.010
G ₃	0.095	0.058	0.124	0.099	0.118	0.224	0.116	0.290
G ₄	0.381	0.144	0.435	0.062	0.386	0.206	0.448	0.175
Relaxation time (min)								
τ ₁	0.950	0.900	0.900	0.830	0.990	0.960	0.990	0.990
τ ₂	8.097	7.980	8.360	8.640	7.970	8.060	8.110	9.900
τ ₃	94.03	89.88	92.64	76.46	93.38	79.06	93.56	70.10
τ ₄	738.0	709.6	709.6	799.3	763.8	747.5	727.3	720.4